PAPER 9 (SESSION I)

The effect of testing system stiffness on fracture behavior of sheet specimens

K. S. GREWAL* and V. WEISS†

*Metallurgist, Syracuse University Research Corporation, Syracuse, N.Y.
†Professor and Associate Chairman, Department of Chemical Engineering and Metallurgy, Syracuse University, Syracuse, N.Y., U.S.A.

Summary

Theoretical analyses and experimental investigations of the stiffness effect on fracture in sheet specimens were carried out. On the basis of notch analysis of fracture in combination with the critical normal stress fracture criterion, notch strength is shown to be a function of testing system stiffness, of the variation of specimen stiffness with crack length, of strain rate, and of crack tip blunting. Based on this analysis, a dimensionless stiffness number, N_s, defined as

$$N_s = -\left(\frac{dP/P}{da/a}\right)_e = -\left(\frac{dU/U}{da/a}\right)_e$$

(where P is the load, a the crack length, U the energy and e the extension of the entire system) is proposed as a measure of testing system stiffness relevant to fracture behavior. An analysis based on the energy criterion of fracture shows that under quasi-fixed grip condition (i.e. extremely slow strain rate), a high stiffness value tends to delay fracture instability, thereby increasing both the notch strength and the critical strain energy release rate. It also predicts that the stiffness effect would be more pronounced for tough materials. Notch strength of fatigue-cracked specimens of several different materials was measured with stiff and dead weight loaded machines. While the notch strength of relatively tough materials was markedly higher in the stiffer system, little or no stiffness effect on notch strength was observed in relatively brittle materials.

Introduction

There is ample evidence that notch strength, fracture appearance, and ductile-brittle transition temperature may be affected by the testing systems stiffness [1-6]. However, there is no consensus about either the magnitude or the significance of this effect [1-8]. No detailed mechanism of the effect has been proposed, nor has any analytical procedure been developed to take system stiffness into account in notch tension or fracture testing. Moreover, most of the work to date was perfomed on steels and little is known about the behavior of other materials.

The objective of this investigation was three-fold. First, to experimentally investigate the effect of testing system stiffness on several different materials over a wide range of stiffness values. Second, to attempt a theoretical analysis of the effect. And third, to outline a procedure for taking this effect into account in notch tension or fracture testing.

Theoretical considerations

Notch analysis provides an elegant means of discussing the effect of testing system stiffness on fracture behavior. According to the critical normal stress fracture criterion, fracture will be initiated when the stress at the crack tip, given by

$$\sigma_{tip} = K_g \sigma_g \tag{1}$$

(where K_g = stress concentration factor based on gross section, and σ_g = gross section stress) reaches a critical value. The rate of change of σ_{tip} with crack length

$$\frac{d\sigma_{tip}}{da} = K_g \frac{d\sigma_g}{da} + \sigma_g \frac{dK_g}{da} \tag{2}$$

yields information regarding the stability of crack growth. If $(d\sigma_{tip}/da) > 0$, cataclysmic crack growth results. If $(d\sigma_{tip}/da) < 0$, crack propagation may change from stable to unstable and the condition

$$\frac{d\sigma_{tip}}{da} = 0 \tag{3}$$

is satisfied at such a transition.

Since

$$\sigma_g = \frac{P}{Bt} = \frac{1}{Bt}\frac{e}{M} \tag{4}$$

where

B = width of the specimen
t = thickness of the specimen
P = load
$e = e_m + e_{sp}$ = extension of the entire system
$M = M_m + M_{sp}$ = compliance of the entire system
e_m, e_{sp} = extension of the machine and the specimen respectively
M_m, M_{sp} = compliance of the machine and the specimen respectively

$$\frac{d\sigma_g}{da} = \frac{1}{BtM}\left[-\frac{e}{M}\frac{dM}{da} + \frac{de}{da}\right] \tag{5}$$

Substituting equation 5 in equation 2, we have

$$\frac{d\sigma_{tip}}{da} = \sigma_g \frac{dK_g}{da} + \frac{1}{BtM}\frac{de}{da} - \frac{e}{BtM^2}\frac{dM_{sp}}{da} \tag{6}$$

On the right side of equation 6, the first term which is positive for brittle behavior [9], may be either positive or negative for the case of plastic flow at the crack tip, the second term is always positive, and the last term (including sign) is always negative (approaching zero in the limiting case of an infinitely soft machine). Thus stable crack growth would be expected, if the strain rate is low, the stiffness is high and the crack tip blunting lowers dK_g/da or possibly makes it negative. When fracture instability is preceded by some stable crack growth under rising load, the factors which favor this slow crack growth will also tend to increase the fracture stress. An expression for fracture stress may be obtained by setting $d\sigma_{tip}/da$ equal to zero. Accordingly

$$\sigma_{gc} = \frac{\dfrac{1}{BtM_c}\left[\dfrac{e}{M_c}\dfrac{dM_{sp}}{da}\Big|_{a=a_c} - \dfrac{de}{da}\Big|_{a=a_c}\right]}{\dfrac{1}{K_{gc}}\dfrac{dK_{gc}}{da}\Big|_{a=a_c}} \tag{7}$$

where a_c, M_c, K_{gc} are the values of crack length, total system compliance and stress concentration factor at instability. Equation (7) not only explains the puzzling experimental observation that the fracture stress increases with increase in system stiffness, but it also brings out the effects of two other relevant factors, namely strain rate and crack tip blunting. The lack of agreement among various investigators concerning the magnitude and significance of the stiffness effect seems to be largely due to different materials, strain rates, and stiffness ranges employed, [1-8].

Multiplying both sides of equation (2) by a/σ_{tip}, we have:

$$\frac{d\sigma_{tip}/\sigma_{tip}}{da/a} = \frac{d\sigma_g/\sigma_g}{da/a} + \frac{dK_g/K_g}{da/a} \tag{8}$$

Since, as shown by equation (5), $d\sigma_g/\sigma_g$ is determined by only system stiffness and its variation with crack length, when the strain rate is vanishingly small, equation (8) suggests that

$$\frac{d\sigma_g/\sigma_g}{da/a}$$

can be used as a meaningful measure of system stiffness. It can be easily shown that for vanishingly small strain rate (we shall call this the quasi-fixed grip condition)

$$\left(\frac{d\sigma_g/\sigma_g}{da/a}\right)_e = \left(\frac{dP/P}{da/a}\right)_e = \left(\frac{dU/U}{da/a}\right)_e \tag{9}$$

where U is the elastic energy of the system and the subscript e refers to the extension of the entire system. Accordingly we define the dimensionless 'stiffness number'

$$N_s = -\left(\frac{dP/P}{da/a}\right)_e = -\left(\frac{dU/U}{da/a}\right)_e \tag{10}$$

as a measure of the testing system stiffness relevant to fracture behavior. The proposed definition of 'stiffness number' in terms of energy is also applicable to a multiaxially loaded specimen.

In order to determine the stiffness number, one needs to know the stiffness of the machine including grips and a relationship between specimen compliance and crack length. Let M_{sp}, M_m, M, and e_{sp}, e_m, e be the compliance and extension values for the specimen, the machine and the total system respectively. By definition

$$e = MP = (M_{sp} + M_m)P \tag{11}$$

Under fixed grip condition for the entire system

$$\frac{de}{dM_{sp}} = (M_{sp} + M_m)\frac{dP}{dM_{sp}} + P = 0 \tag{12}$$

or

$$\frac{1}{P}\frac{dP}{dM_{sp}} = -\frac{1}{M}$$

Therefore

$$N_s = -\frac{dP/P}{da/a} = \frac{a}{M}\frac{dM_{sp}}{da} \tag{13}$$

It will be shown below that the stiffness number is also relevant to the analysis of stiffness effect in terms of the energy criterion for fracture instability [10-12] i.e.

$$\frac{dG}{da} \geqslant \frac{dR}{da} \tag{14}$$

Where G is the strain energy release rate and R the crack-extension resistance. Assuming fixed grip condition for the entire system

$$G = -\frac{dU}{da} = -\frac{d}{da}(1/2\ eP) \tag{15}$$

and

$$\frac{dG}{da} = -\frac{d^2U}{da^2} = -\frac{e}{2}\frac{d^2P}{da^2} \tag{16}$$

Differentiating $P = e/M$ twice with respect to a, under the same assumption gives

$$\frac{d^2P}{da^2} = \frac{2e}{M^3}\left(\frac{dM_{sp}}{da}\right)^2 - \frac{e}{M^2}\frac{d^2M_{sp}}{da^2} \tag{17}$$

Substituting this expression for d^2P/da^2 in equation (16)

$$\frac{dG}{da} = -\frac{d^2U}{da^2} = \frac{e^2}{a^2M}\left[\frac{a^2}{2M}\frac{d^2M_{sp}}{da^2} - N_s^{\,2}\right] \tag{18}$$

Substituting for dG/da in the instability condition, equation (14), we have

$$\frac{e^2}{a^2M}\left[\frac{a^2}{2M}\frac{d^2M_{sp}}{da^2} - N_s^{\,2}\right] - \frac{dR}{da} \geqslant 0 \tag{19}$$

Equation (19) shows that a high stiffness number and a high value of dR/da, both tend to delay fracture instability. dR/da generally decreases with increase in crack length [11,12]. Thus if the instability condition is not fulfilled in the beginning because of high dR/da, stable crack growth will occur, usually under increasing load, until dR/da decreases to satisfy equation (19). The higher the stiffness number, the lower will be the value of dR/da at instability. Thus a high stiffness number will tend to increase the fracture stress, the critical strain energy release rate and the amount of stable crack growth. Equation (19) also shows that for tougher materials (i.e. high initial value of dR/da) stiffness effects will be more pronounced because with high dR/da, the term containing $N_s^{\,2}$ becomes larger in proportion to the rest of the expression on the left of equation (19).

Experimental procedure

Load-extension curves for center-cracked or single edge-cracked specimens were obtained for various values of system stiffness. Specimen designs are shown in Fig. 1. Table 1 gives the specimen types and test conditions for the materials investigated.

All of the specimens contained fatigue cracks produced by extending initial jeweler's saw cuts by tension-tension fatigue. Ti RS-140 specimens were cracked before austenitizing to minimize structural changes caused by cracking and to facilitate precise measurement of initial crack length after fracture. The center-cracked specimens, which were machined oversize by 0·25 in, were finish machined after fatigue cracking such that the crack was symmetrical with respect to the edges.

The grip portions of the center-cracked specimens were stiffened by 0·125 in thick steel plates, bonded on both sides with Hysol 4321 epoxy cement. Pin-loaded grips were used in all cases.

In order to study the effect of specimen thickness, short single edge cracked specimens (Fig. 1 (b)) of Al 2024-T351 were reduced only over the gage length to 0·125 and 0·063 inch in thickness.

Four different testing machines were used: 10,000 lbs. capacity Instron (screw driven), 60,000 lbs capacity Baldwin (hydraulic), a lever type dead weight loaded machine and a specially constructed stiff machine, screw driven with a solid state strain gage load cell [13, 14]. Typical stiffness values of these machines were ·5, ·4, 0 and 2 million lbs/in, respectively. Additional stiffness ranges were obtained by incorporating springs or suitable linkage in the Baldwin machine. Specimens were strained very slowly to approximate the quasi-fixed grip condition assumed in the analysis; extension rates ranged for 0·001 in to 0·003 in/min.

Experimental results and discussions

Experimental results on all three types of specimens indicate that stiffness effects are more pronounced in a relatively ductile and tough materials. No effect of testing system stiffness was observed on center-cracked specimens of Ti RS 140 in relatively brittle temper i.e. aged at 700 and 900°F, Fig. 2. However, in the relatively tough solution treated condition this material showed a small but definite stiffness effect, Fig. 2.

Tests on long single edge notch specimens again showed pronounced stiffness effect in relatively tough AISI 4340 specimens and little effect in less tough Al 7075-T6 specimens, Fig. 3.

Tests on short single-edge notch specimens showed less stiffness effects in type 301 Stainless Steel 60% cold reduced, than in Al 2024 specimens, Fig. 2, However, these data cannot be interpreted on the basis of toughness difference alone, which is probably quite small. Another factor may be the higher stiffness number for the system with Al 2024-T3 specimens.

The difference in notch strength between specimens tested in the stiff and the dead weight loaded machines decreased with increase in thickness, Fig. 4. This effect also cannot be entirely attributed to higher stiffness number for the system with thinner specimens, because shear fraction of fracture surface also increased with decrease in thickness; the fracture surface of the 0·063 in specimen being 100 percent shear while that of 0·25 in specimen being almost flat. This change in fracture toughness with thickness is primarily responsible for the variation in notch strength obtained with dead weight loaded machine. Thus the enhanced stiffness effect for the thinner specimens is due to variation in both stiffness number and fracture toughness with specimen thickness.

With the exception of type 301 stainless steel and Al 2024 specimens, fracture appearance was not affected by the testing system stiffness. Fracture in Ti RS 140 and AISI 4340 steel was always shear type and in Al 7075-T6, always flat. Although the fracture appearance of type 301 stainless steel was 100 percent shear in both stiff and dead weight loaded machines, the fracture path was oblique in the case of specimens tested in the stiff machine. For Al 2024 specimens, percent shear was greater in specimens tested in the dead weight loaded machine than in those tested in the stiff machine.

A similar effect was observed by Puttick, who was able to suppress the shear portion of the cup and cone fracture in an Armco iron specimen by using a hard machine [15]. Following Zener [16], Cottrell attributed Puttick's observation to elimination of adiabatic shear in a hard machine [17]. However according to Rogers [18], even the normal fracture is of shear type on a small scale and appears flat because the crack propagates in small steps and cannot leave the plane of maximum normal stress

in a hard machine. In a soft machine, there is plenty of stored energy in the system and crack leaves the plane of maximum stress at an early stage Since the metallographic examination of transverse sections did not reveal any evidence of gross adiabatic shear, we tend to agree with Rogers' interpretation.

The effect of testing system stiffness on fracture behavior of a specimen has two aspects. The first is the stiffness of the system and its change with crack length. The second is the response of the specimen material to the first. The latter depends on specimen thickness and material characteristics such as ductility and strain-hardening behavior. The former can be best characterized by the stiffness number, N_s, which is a function of testing system stiffness and its variation with crack length. At present, it is not possible to give a detailed analysis of the material response. However, if one plots some material property susceptible to the effect of testing system stiffness, such as notch strength, against N_s, one has a quantitative basis of comparing differing materials regarding their response to testing system stiffness. Fig. 3 gives such a plot for Al 7075-T6 and AISI 4340 steel.

Conclusions

1. On the basis of notch analysis of fracture in combination with a critical normal stress fracture criterion, it is shown that the notch strength can be affected by the stiffness of the testing system. The effect increases with a decrease in strain rate. Crack tip blunting is suspected to be an important factor in the stiffness effect.

2. Based on the above analysis, a dimensionless stiffness number

$$N_s = \left(\frac{dP/P}{da/a}\right)_e = \left(\frac{dU/U}{da/a}\right)_e$$

is proposed as a significant measure of system stiffness.

3. An analysis based on the energy criterion of fracture shows that under quasi-fixed grip condition (i.e. extremely slow strain rate), a high stiffness number tends to delay fracture instability, thereby increasing both notch strength and critical strain energy release rate. It also predicts that the stiffness effect would be more pronounced for tough materials in which resistance to crack propagation rises rapidly with crack growth.

4. While the notch strength of relatively tough materials was markedly higher in the stiffer test system, little or no stiffness effect on notch strength was observed in relatively brittle materials.

Acknowledgements

The authors wish to acknowledge the financial support of this investigation by the Air Force Materials Laboratory through contract No. Af 33

(615) - 1602. We are also indebted to W. Rosenberg and H. Lin for technical assistance and to C. Libove and J. Sessler for helpful discussions.

References

1. DE LEIRIS, H. 'On the influence of length on the phenomenon of semi-brittle fracture', *Comptes Rendus des Acad. de Sciences*, Vol. 234, pp. 1125-1126, 1952.
2. DE LEIRIS, H. *Bull. Soc. Francaise des Mec.*, Oct., 1952.
3. TIPPER, C. F. West of Scotland Iron and Steel Institute, Conference on Brittle Fracture, p. 458, 1953.
4. TIPPER, C. F. *Brit. Weld. J.*, Vol. 3, p. 435, 1956.
5. ALMAR-NAESS, A. 'Influence of external energy on brittleness in bend tests', *Brit. Weld. J.*, Vol. 4, p. 88, 1957.
6. BALL, R. E. M. & TURNER, C. E. 'Some effects of external energy on fracture in the notch tensile test of mild steel,' *J. Iron and Steel Inst.*, Vol. 201, pp. 47-53, 1963.
7. SAVITSKY, F. S. & VANDYSLEV, B. A. *Zavods. Lab.*, Vol. 22, p. 717, 1956.
8. BUCHER, J. H., CAMMETT, J. T., JASPER, J. C., POWELL, G. W. & SPRETNAK, J. W. 'The relationship of microstructure to strength and toughness in high strength steel', *Air Force Materials Laboratory Report No. AFML-TR-65-60*, 1965.
9. DIXON, J. R. 'Stress distribution around a central crack in a plate loaded in tension; effects of finite width of plate,' *J. Roy. Aero. Soc.*, Vol. 64, pp. 141-145, 1960.
10. IRWIN, G. R. 'Fracture of high strength sheet materials under conditions appropriate for stress analysis', *U.S. Naval Res. Lab. Report 5486*, July, 1960.
11. KRAFFT, J. M., SULLIVAN, A. M. & BOYLE, R. W. 'Effect of dimensions on fast fracture instability of notched sheets,' Proceedings, Crack Propagation Symposium, College of Aeronautics, Cranfield, England, Vol. 1, pp. 8-28, 1961.
12. BROWN, W. F. & SRAWLEY, J. E. 'Fracture toughness testing', in book Fracture toughness testing and its applications, *Am. Soc. Test. Mats. Special Technical Publication No. 381*, pp. 133-196, 1965.
13. WEISS, V., GREWAL, K., ROSENBERG, W. & LIN, H. 'The effect of testing system stiffness on fracture behavior of sheet specimens', *Air Force Materials Laboratory Report No. AFML-TR-37, 1967.*
14. GREWAL, K. S. 'The effect of testing stiffness on fracture behavior of sheet specimens', *Ph.D. Dissertation, Syracuse University*, 1967.
15. PUTTICK, K. E. 'The shear component of ductile fracture', *Phil. Mag.*, Vol. 5, pp. 759-762, 1960.
16. ZENER, C. 'The micro-mechanism of fracture', in *'Fracturing of Metals'*, *American Society Metals*, pp. 3-31, 1948.
17. COTTRELL, A. H. 'Theoretical aspects of fracture', in *Fracture*, edited by Averbach *et al.*, John Wiley and Sons, Inc.: New York, pp. 21-53, 1959.
18. ROGERS, H. C. *ibid.*, pp. 46-49.

Table 1
Materials, specimen types and test conditions

Materials	*Specimen type*	*Thickness in*	*Gage length in*	*Testing machines*
Ti-RS 140 aged 6 hrs at 700°F [1]	Fig. 1 (a)	0·025	4	Stiff and dead weight loaded
Ti-RS 140 aged 6 hrs at 900°F [1]	Fig. 1 (a)	0·025	1	Stiff and dead weight loaded
Ti-RS 140 solution treated [1]	Fig. 1 (a)	0·025	1	Stiff and dead weight loaded
Type 301 stainless steel 60% cold. red. [2]	Fig. 1 (b)	0·063	0·5	Stiff and dead weight loaded
Al 2024-T3[3]	Fig. 1 (b)	0·125	0·5	Stiff and dead weight loaded
Al 2024-T351 [3]	Fig. 1 (b)	0·250 0·125 0·063	0·5	Stiff and dead weight loaded
Al 7075-T6 [4]	Fig. 2	0·250	5·5	Stiff, Instron, Baldwin with spring in series with specimen, Dead weight loaded
AISI 4340 steel tempered 900°F [5]	Fig. 2	0·125	4	Stiff, Instron, Baldwin with spring in series with specimen, Dead weight loaded

1. 5·10 Al, 3·10 Cr, 1·30 Fe, 0·030 C, 0·011 N (Actual analysis)
2. 17 Cr, 7 Ni, < 0·15 C, < 2·00 Mn, < 1·00 Si
3. 4·5 Cu, 1·5 Mg, 0·6 Mn (Nominal Composition)
4. 5·5 Ln, 2·5 Mg, 1·5 Cu, 0·3 Cr (Nominal Composition)
5. 0·40 C, 1·74 Ni, 0·81 Cr, 0·26 Mo, 0·75 Mn, 0·31 Si, 0·015 S, 0·009 P (Actual analysis). All figures are percentages by weight

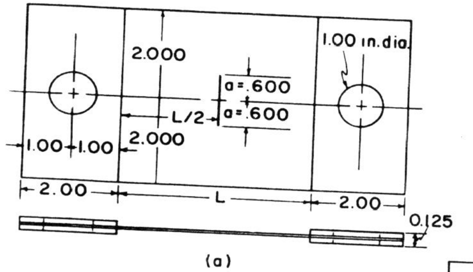

	A	B	C	D	E	F	G	H	I	J
Al-7075-T6	9	4	1	1	$\frac{3}{4}$	$1\frac{1}{2}$	1	$\frac{3}{16}$	4	8
AISI 4340	6	3	1	1	$\frac{1}{2}$	1	1	$\frac{3}{16}$	$5\frac{1}{2}$	$11\frac{1}{4}$

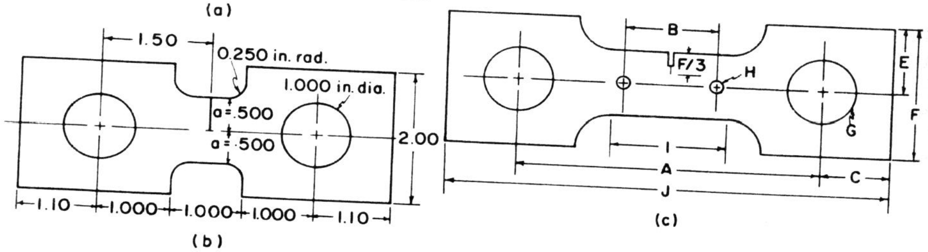

Fig. 1. Design of (a) Center-crack, (b) Short single edge-crack and (c) Long single edge-crack specimen.

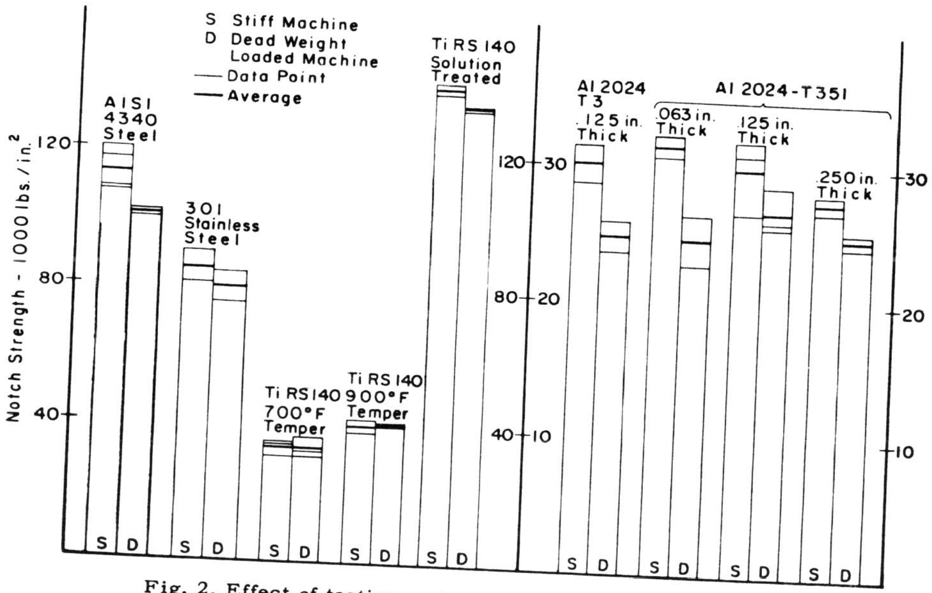

Fig. 2. Effect of testing system stiffness on notch strength.

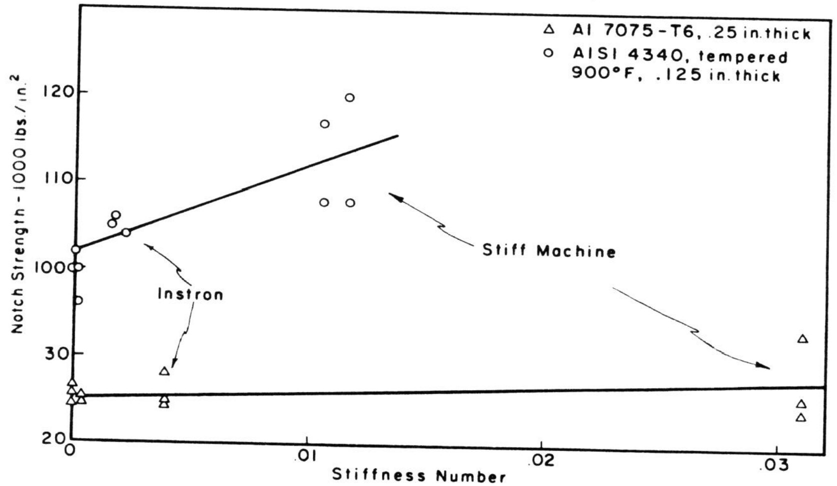

Fig. 3. The effect of stiffness number, N_s, on notch strength of Al-7075-T6 and AISI 4340 tempered at 900°F.

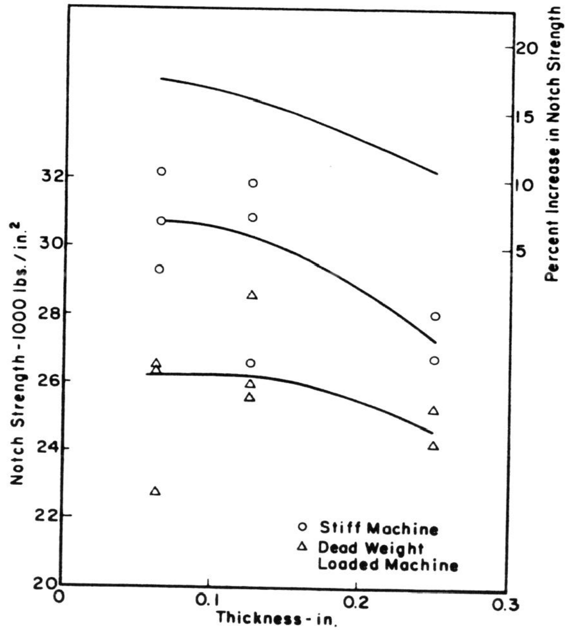

Fig. 4. Effect of thickness on notch strength of Al 2024-T351 specimens.